Sol-gel synthesis and properties of nanocomposites in the $Ag/TiO_2/ZnO$ system

A. SHALABY[a,b], A. BACHVAROVA-NEDELCHEVA[c], R. IORDANOVA[c], Y. DIMITRIEV[b], A. STOYANOVA[d], H. HITKOVA[d], N. IVANOVA[d], M. SREDKOVA[d]
[a]*STCE – Science and Technology Center of Excellence, Cairo-Egypt*
[b]*University of Chemical Technology and Metallurgy, 8 Kl. Ohridski blvd., 1756 Sofia, Bulgaria*
[c]*Institute of General and Inorganic Chemistry, Bulgarian Academy of Sciences, G. Bonchev str., bld. 11, 1113 Sofia, Bulgaria,*
[c]*Medical University, 5800 Pleven, Bulgaria.*

Composite powders with initial components Ag, TiO_2 and ZnO were prepared by sol-gel processing containing titanium ethoxide, silver nitrate and zinc acetate as precursors in an Ag/Ti/Zn atomic ratio of 1:2:3. The as-obtained gels were stepwise calcinated up to 600^0C. The phase and structural transformations at every step of the heat treatment were followed by X-ray phase analysis. The amorphous phase which is dominant up to 300ºC decreases gradually with increasing the temperature, while elementary silver, ZnO and cubic $ZnTiO_3$ coexist simultaneously in a nanocomposite at 500ºC. At 600^0C the crystallinity of the sample increased and the amount of amorphous phase is small enough to be negligible. The average particle size of $ZnTiO_3$ increases from 6 to 10 nm, of elementary silver – 25 nm and ZnO – 24 nm in the range 500-600^0C. The obtained $Ag/ZnO/ZnTiO_3$ composite showed photocatalytic activity toward Malachite Green (MG) under ultraviolet and visible light irradiation. The antibacterial activity was examined in the dark and under UV-light using as a test-microorganism *Escherichia coli* ATCC 25922. The obtained nanocomposite possesses a powerful bactericidal effect and can completely kill *E. coli* bacteria after 30 minutes. A simple scheme for performance of a complex composite containing three active phases was suggested.

(Received June 25, 2014; accepted January 21, 2015)

Keywords: Sol-gel, Ag/ $ZnO/ZnTiO_3$ composite, Photocatalyst, Antibacterial properties

1. Introduction

In the past years, TiO_2 and ZnO materials received special attention due to their unique optical, electrical and chemical properties. From a practical point of view, titanium oxide (TiO_2) has been recognized as the preferable one for photocatalytic degradation of organic pollutants and other environmental applications due to its high photosensitivity, strong oxidizing power, nontoxic nature, and chemical stability [1-6]. Zinc oxide (ZnO) is an alternative to TiO_2 because its electrical, optical, photocatalytical behaviour has been proven to be similar [7, 8]. Several prioritised and more detailed investigations for the degradation of organic dyes by ZnO (nanoparticles and thin films) have been performed [9-12]. In an important paper of Marci et al. [13] it was found that ZnO considerably enhances the photocatalytical performance of TiO_2 under UV irradiation and many studies have been focused on the binary TiO_2/ZnO compositions. During the investigation, three compounds $ZnTiO_3$, $Zn_2Ti_3O_8$ and Zn_2TiO_4 were found in the ZnO-TiO_2 system [14, 15]. Among them, the zinc titanate ($ZnTiO_3$) is a well known functional inorganic material due to its numerous applications in industry (paint pigment, catalytic sorbent, sensor). Recent studies also confirmed that it is a good dielectric ceramic material [16-20] and it can be a useful candidate for low-temperature cofired ceramics [21]. Due to its photocatalytic properties it is of some increased interest for degradation of organic pollutants [22-25]. For these applications, appropriate strategies for preparation were developed including conventional solid state reactions [26], mechanical activation [18] and several variants of sol-gel methods [19, 20, 23, 25-31].

In order to improve the electronic properties of the materials from the ZnO-TiO_2 system, especially the absorbance under visible irradiation, many other dopants instead of ZnO have been studied also, such as: noble metals, transition metal cations, lanthanides cations, anions of non-metal elements, which have been introduced by oxides, salts, sulfides, halcogenides or more complex compounds [1, 4, 7, 32]. Among the different investigated dopants, silver was recognized as playing a positive role in trapping the photo-generated electrons, retaining the recombination processes (e^-/h+ pair) realizing appropriate charge separation. In this way it contributes to the improvement of photocatalytical and antibacterial properties. Some of the earlier studies with positive results (concerning the photocatalytic activities of silver doped

TiO_2) were reviewed by Han et al. [33]. In the last ten years, this topic continues to be very attractive. For the preparation of such composites, several methods have been proposed: sol-gel method [34-45], co-sputtering [46], liquid impregnation [47, 48], photodeposition [49, 50], photoreduction [51], electrochemical technique [52], spray pyrolysis [53], electrospinning technique [54] mechanical ball milling [55], dip-coating method [44, 56]. The content of silver in the pointed above studies varies from 0.1 [42] to 10 % [35] depending on the tasks which had to be solved. That is why it is difficult to accept only one optimal concentration. For example good photocatalyst is obtained when the molar ration Ag/Ti is 1:9 [40], while small amounts of silver doped TiO_2 thin films were successfully applied for self-cleaning processes and indoor air pollution treatments [42]. Most of the materials obtained by the above indicating methods have been successfully applied for the purification of water solutions from organic pollutants: toward degradation of Rhodamine B (RdB) [35], AR88 [48], Methyl orange (MO) [52, 54, 55], Methylene blue [33, 42], Reactive black [49], acid orange [50], some gaseous pollutants – formaldehyde, xylem, benzene [39, 42] and nalidixic acid degradation [45]. Silver doped TiO_2 nanocomposites showed excellent antibacterial capability against *E. coli* and other microorganisms [38, 41, 43, 51, 57, 58]. A similar behaviour to those of Ag/TiO_2 composite has been established recently in a number of papers for Ag/ZnO modified powders [59-72] and films [73, 74]. They have been applied mainly for photocatalytic performance [59, 63, 65, 66, 67, 72, 73] and antibacterial applications against *E. coli, P. putida, S. aeruginosa,* and other [61, 62, 64, 66, 67, 68, 69, 70, 74]. From the above brief review it is seen that irrespective of numerous published papers, the interest concerning photocatalytical and antibacterial active materials continue to increase, due to the demand and necessity to obtain practically useful products. This is connected with the development of more effective methods of preparation, because they determine the properties of materials. Up to now, data for impregnation, precipitation, mechanochemistry, sonochemistry, hydrothermal route were published, but among them the most popular is the sol-gel technique. A new tendency is observed in the last studies connected with the preparation of complex multifunctional materials containing several active components, the so called "synergetic effect" [78]. Recently, promising results have been published for Ag/ZnO/TiO_2, Ag/Zn_2TiO_4 and Au/ZnO/TiO_2 [54, 75-77]. This is a strategy for solving the problems of waste waters simultaneously containing many different organic pollutants.

Most of our previous studies of materials in the ZnO-TiO_2 system have been performed in the framework of a project titled "Synthesis of nanostructred ZnO for photocatalytical applications" in the period 2007-2010. Several sol-gel methods were applied for synthesis of nanopowders: aqueous [79-83], non-aqueous sol-gel [84], combustion [85, 86] and mechanochemical synthesis [87]. Investigations were made also on ZnO and ZnO/TiO_2 films for the photocatalytical applications [88-91]. All obtained materials possess photocatalytical activity against Malachite green dye chosen as a typical organic water pollutant. For the first time it was shown that pure $ZnTiO_3$ possesses strong antimicrobial activities against a high concentration of *E. coli* bacteria [81]. These results, as well as those published by many authors about active materials with participation of ZnO and TiO_2 motivate us to continue investigations on this topic. The present paper is focused on studying a new combination of components in the Ag-TiO_2-ZnO system.

Applying a sol-gel method, we made an attempt to obtain a nanocomposite material containing several active phases, to study its phase transformations by increasing the temperature, to elucidate the influence of the amorphous phase, particles size distribution and to verify its photocatalytical and antibacterial properties.

2. Experimental

2.1 Samples preparation

The main stages for sol-gel synthesis of the powders are shown in figure 1. For the synthesis of the Ag/TiO_2/ZnO sample, the atomic ratio 1:2:3 between the components was chosen and analytically pure precursors were used: titanium ethoxide [$Ti(OCH_2CH_3)_4$] (Fluka AG), zinc acetate, $Zn(CH_3COO)_2.2H_2O$ (Merck), ethylene glycol ($C_2H_6O_2$) (Merck), ethyl alcohol (C_2H_5OH) (Merck) and citric acid monohydrate ($C_6H_8O_7.H_2O$) (Merck), NH_4OH (25% NH_3) (Merck) and silver nitrate ($AgNO_3$-Fluka AG). The silver nitrate was dissolved in C_2H_5OH and then ammonia solution was added dropwise in order to make the solution clear and to control the pH (~ 6-7) as well. The citric acid was used as a main chelating agent because it is well known that it stimulates the gelation process due to the strong coordination ability of metal ions with citrate groups [92]. The solutions were subjected to 5 - 10 min intensive stirring at room temperature in order to achieve complete dissolution. As prepared solutions were mixed and homogenized for 15 min at 60-80^{0}C. The gelation process took between 5-15 min and the aging was performed in air for several days at room temperature. The as obtained gels were subjected consequently to evaporation in a water bath, drying on a hot plate and calcinated at 400, 500 and 600^{0}C for 1h exposure time in air. The selection of temperatures was made having in mind our previous experiments on the ZnO-TiO_2 system [79-81].

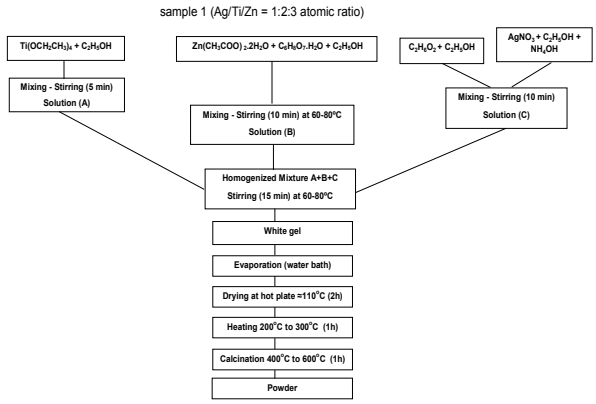

Fig. 1. Scheme for synthesis of a composite in the Ag/TiO_2/ZnO system with Ag/Ti/Zn atomic ratio 1:2:3

2.2 Samples characterization

The phase formation processes were followed by Bruker D8 Advance X-ray apparatus, Cu Kα radiation in the range from 10 to 80° 2θ with a step 0.02 and scanning time of 0.1 sec. The particles morphology of the calcinated at 300 and 600^{0}C powders was observed by Scanning Electron Microscopy (JEOL Superprobe 733). The optical absorption spectra of the powdered samples in the wavelength range 200–1000 nm were recorded by a UV–VIS diffused reflectance Spectrophotometer "Evolution 300" using a magnesium oxide reflectance standard as the baseline. The uncertainly in the observed wavelength is about ±1 nm. The absorption edge and the optical band gap were determined following Dharma et al. instruction [93], which were applied recently in numerous papers [25, 94, 95]. The bandgap energies (E_g) of the samples were calculated by the Planck's equation: $E_g = \frac{h.c}{\lambda} = \frac{1240}{\lambda}$, where Eg is the bandgap energy (eV), h is the Planck's constant, c is the light velocity (m/s), and λ is the wavelength (nm) [78].

2.3 Photocatalytic activity experiments

The photocatalytic activity tests were made following a well known procedure described in details elsewhere [96]. The photocatalytic activities of the synthesized powders were assessed by the degradation of the organic dye Malachite Green (MG), as a model pollutant. In a typical procedure 100 mg of the investigated sample was added to 150 ml dye solution (5 ppm) to form a suspension. Prior to irradiation, the suspensions were sonicated for 10 min, and then stirred in the dark for 30 min to ensure the establishment of adsorption/desorption equilibrium. The UV-irradiation was carried out using a black light blue lamp (Sylvania BLB 50 Hz 8W T5). The visible light source was a 500 W halogen lamp (Sylvania). Aliquot samples of the mixture (3 mL) were withdrawn before and at different time intervals during the irradiation and centrifuged in order to remove the solid particles. The change in the dye concentration in each aliquot was determined by measuring the absorbance value at 620 nm using Jenway 6505 UV-Vis spectrophotometer. The indicated experimental conditions were selected bearing in mind our previous investigation [82, 84] in order to make the obtained results comparable.

2.4 Antibacterial activity testing

A stock culture of *Escherichia coli* ATCC 25922 was streaked on a blood agar plate. After overnight incubation, one cell colony was subcultured in 50 ml nutrient broth for 15 h at 37°C. The liquid culture was then centrifuged at 1000xg for 10 min, washed twice with sterile PBS (pH 7.2) and resuspended. The obtained suspension was adjusted to 0.5 Mc Farland using the densitometer (Densimat, bioMerieux) and afterwards diluted 1000 times to prepare turbidity corresponding to 10^5 colony forming units per milliliter (CFU/ml). The experimental set up, as previously described [81, 82], consisted of sterile glass flasks each with 100 ml bacterial suspension with an initial cell density approximately 10^5 CFU/ml. The first flask served as a control of bacterial growth. The second flask, containing 100 mg of sample 1, was kept in the dark by wrapping with aluminum foil. The third flask, also with 100 mg of sample 1, was illuminated with UV-A light (lamp Sylvania, BLB, 50 Hz, 8W, T5 with major fraction of 365 nm) situated sidewise at a distance of 10 cm. The experiment was carried out at room temperature with constant stirring for 1 hour. Aliquot samples were collected from each flask every ten minutes and once after keeping 24 h in dark conditions. Subsequently serial ten-fold dilutions were prepared and 100 μl of proper dilutions were spread immediately on 3 agar plates (Mueller-Hinton agar, BD Microbiology Systems). The plates were then cultivated at 37°C in an incubator. After overnight incubation, the number of viable bacteria was detected by counting the colonies and calculating per 1 ml. The results are presented as survival curves.

3. Results and discussion

3.1 Phase characterization of the composites

The XRD patterns of annealed at 300, 500 and 600^{0}C samples with the Ag/Ti/Zn atomic ratio 1:2:3 are presented in Fig. 2. The other data for intermediate temperatures was not presented because new phase transformations were not registered. At 300^{0}C, typical interplanar distances for metallic silver with 2θ values at 38.12; 44.28; 77.47 (JCPDS 04-0783), ZnO with 2θ values at 36.25; 31.77; 34.42 (JCPDS 36-1451) and an amorphous halo for amorphous phase were detected. The strongest diffraction peaks with 2θ values at 35.38; 30.03; 62.45 (JCPDS 39-0190) appeared for cubic $ZnTiO_3$ at 500 and 600^{0}C, along with metallic silver and ZnO. As it is seen, at 500^{0}C the presence of the amorphous phase decreases and at 600^{0}C is negligible. The XRD patterns of a reference Ag/TiO_2

sample (atomic ratio 1:9), at 300^{0}C exhibited separation of metallic silver and TiO_2 (anatase) (JCPDS 04-0783) and at 500 and 600^{0}C started the crystallization of TiO_2 (rutile) (JCPDS 89-0555). Having in mind the existence of several phases in the TiO_2-ZnO phase diagram and to verify the stability of $ZnTiO_3$, an additional heat treatment at 800^{0}C was performed. At this temperature, the diffraction peaks with 2θ at 35.16; 29.86; 62.07 of Zn_2TiO_4 (JCPDS 19-1483) were detected. That is why the experiment was limited up to 600^{0}C.

The average crystallite size of the silver nanoparticles, calculated from the broadening of the strongest silver diffraction line (2θ = 38.12, hkl = 111) (samples at 300^{0}C) using Sherrer's equation is 25 nm, for ZnO is near 24 nm and for $ZnTiO_3$ varies from 6 to 10 nm. A comparison of our results with those obtained by other authors for similar systems, showed some differences due to the peculiarities of applied method of synthesis, selected compositions and influence of silver. According to Zhang et al. [97] pure TiO_2 is amorphous up to 400^{0}C, Gupta et al. [43] as well as Hsieh et al. [58] observed that the crystallization of rutile crystal phase occurred after 400^{0}C. Seery et al. [37] established anatase to rutile phase transformation at a higher temperature (above 600^{0}C). In ZnO based thin films a mixture of an amorphous phase and crystallites with average particles size 9-15 nm at 200^{0}C was found [98, 99]. Moreover, for Ag/ZnO composite obtained by a one-step impregnation method the appearance of wurtzite crystals even at room temperature is reported [70]. Pant et al. [75] established that in an Ag/TiO_2/ZnO composite heat treated up to 140^{0}C, formation of ZnO and silver metal is registered. According to our previous investigations [79] the crystallization of ZnO started at 200^{0}C (sol-gel method) with average particle dimensions above 100 nm. On the other hand, in the pure $ZnTiO_3$ synthesized by us the amorphous phase is preserved up to 500^{0}C [80, 81]. From the above mentioned results it may be concluded that doping of TiO_2 or ZnO with silver led to enhancement of crystallization processes, but TiO_2 is more stable against crystallization than ZnO and the amorphous phase was detected up to 500^{0}C in the composite (Fig. 2). The TiO_2 crystal phase was not found and the final composite consists of Ag, ZnO and $ZnTiO_3$ (at 600^{0}C).

Fig. 3a, b shows the SEM image of the morphology of the sample heat treated at 300 and 600^{0}C. Small pieces 0.2 – 1 mm are observed as a result of the crashing of the monolithic gel. On their amorphous-like surface, bright small aggregates probably due to the silver are randomly distributed with the average particles size below 1μm (Fig. 3a). At 600^{0}C the size of aggregates increased (Fig. 3b).

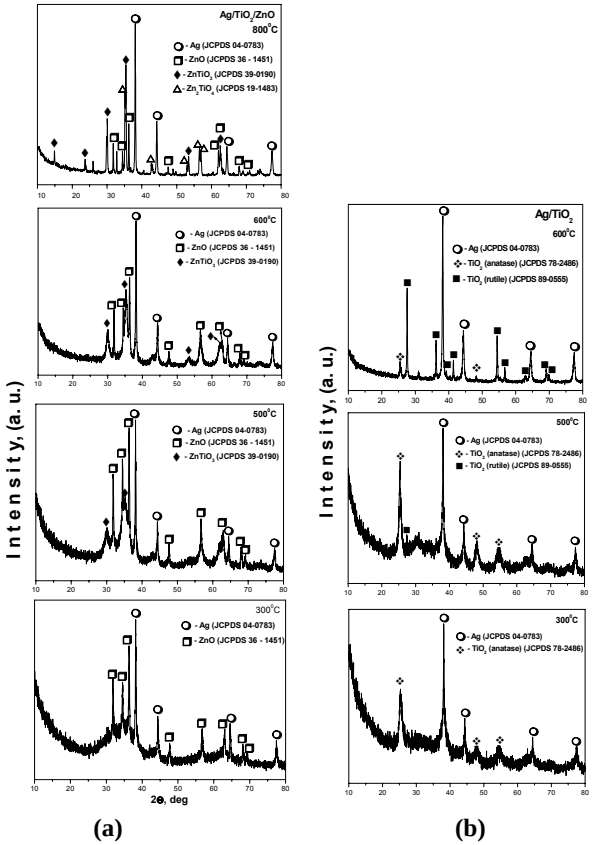

Fig. 2. X-ray diffraction patterns of Ag/TiO_2/ZnO sample (a) and reference Ag/TiO_2 sample (b) heat treated at different temperatures

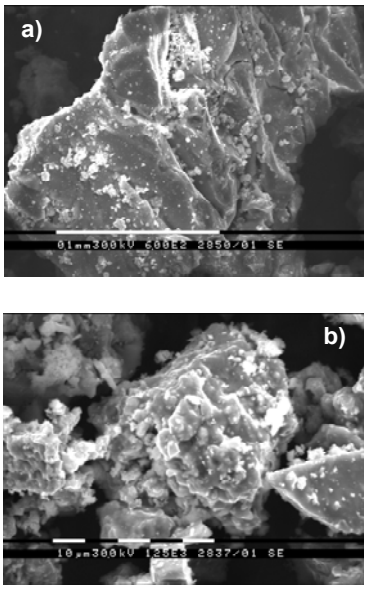

Fig. 3. SEM images of the sample heat treated at 300^{0}C (a)and 600^{0}C (b)

3.2 UV-Vis diffuse reflectance spectra

Fig. 4 shows the absorption spectra for the sample annealed at 300 and 600^{0}C. A decrease of absorption above 400 nm at both temperatures is observed. The absorption edge at 300^{0}C is 409 nm which slightly moved to a longer wavelength - 416 nm, after annealing at 600^{0}C. An increase of the absorption is observed in the visible region about 500 nm that could be due to the surface plasmon resonance effect of separated silver nanoparticles [58, 74, 100]. The calculated band gap values (Eg) negligible decreased from 3.03 to 2.98 eV after crystallization at 600^{0}C. For comparison, the band gap values of different materials are shown below: Degussa P-25 (3.1 eV) [101], amorphous TiO_2 (3.4-3.5 eV) [94, 97, 102]; Ag/TiO_2 is 2.7-2.9 eV [42], 2.9-3.2 eV [58], 2.7-2.8 eV [43], 3.17 eV [74], pure ZnO - 3.27-3.3 eV [25, 70, 95], and Ag/ZnO composites are 3.18-3.19 eV [74], 3.09 eV [70], 3.14 eV [63], 3.17 eV [72]. The optical band gap for pure $ZnTiO_3$ was found 2.7-2.9 eV [103, 104]. The band gap sizes reach a maximum in the amorphous TiO_2 sample ($TiO_2.nH_2O$) [97]. The amorphous phase in ZnO films deposited at low temperature is characterized by the blueshift of optical band gap [98]. According to Kaur et al. [105] the relatively large band gap of amorphous TiO_2 in respect to rutile and anatase, suggests that it is photocatalyticaly less efficient than the crystalline forms. The problem concerning the exact influence of amorphous phase on the photocatalytical properties is still disputable because many factors act simultaneously [94]. Obviously, more experiments are necessary in order to solve that problem. Incidentally, as was mentioned in the literature, the preparation of amorphous TiO_2 and ZnO is cheaper and easier for performance [94, 97, 105].

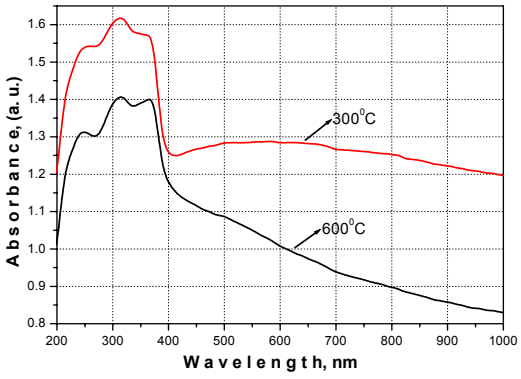

Fig. 4. UV-Vis absorption spectra of the sample at 300 and 600^{0}C.

3.3 Photocatalytic activity

The results for the photocatalytic decoloration of MG by Ag/ZnO/$ZnTiO_3$ composite (600^{0}C) under visible and ultraviolet irradiation are shown in Fig. 5. As can be seen, the decolouration increases faster in comparison to the pure $ZnTiO_3$. The positive effect of introducing Ag into TiO_2/ZnO system is evident under both – UV and visible light irradiation. In 120 minutes the C/C_0 value is near 0.3 for the composite, while for pure $ZnTiO_3$ the same value is achieved in 180 minutes [82]. According to Pant et al. [75] the Ag/TiO_2/ZnO composite (heated up to 140^{0}C) decolourized Reactive Black organic dye in 210 minutes under UV irradiation. The similar effect of silver in combination with TiO_2 and ZnO was also found for the CO_2 photoreduction [74]. The results for photocatalytical behavior (Fig. 5) could be explained by the synergetic effect of the participating components metallic Ag, ZnO and $ZnTiO_3$ (Fig. 2a). The theoretical explanation of the processes is discussed in several papers and it is connected to the retaining of recombination, which might be attributed to the high separation efficiency on the photo generated e^-/h^+ pairs [33, 54, 64, 74].

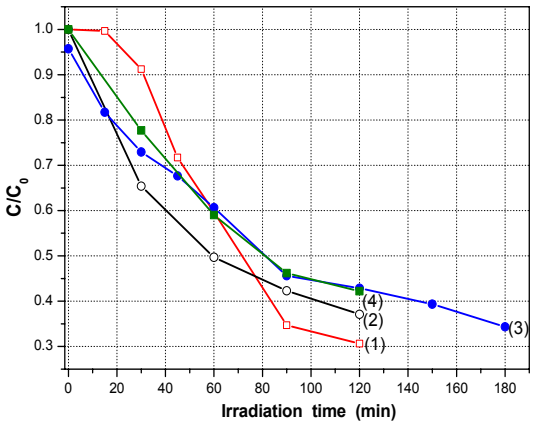

Fig. 5. Photocatalytic decoloration of MG water solutions by Ag/ZnO/$ZnTiO_3$ composite (600^{o}C) under UV (1) and Vis (2) light irradiation and pure $ZnTiO_3$ under UV (3) [82] and Vis (4) light irradiation

3.4 Antibacterial test

The results from antibacterial testing of UV illuminated and non-illuminated Ag/ZnO/$ZnTiO_3$ composite (600^{0}C) are presented at Figure 6. As can be seen the illuminated powder effectively killed *E. coli* in 20 min and the number of cells has decreased from 1.82×10^5 CFU/ml to 3.52×10^3 CFU/ml, the reduction index is 98%. The non-illuminated sample with an identical cell count exhibited antibacterial action - 93.54% reduction of bacteria in the same time frame (20 min). The subcultures from illuminated and non-illuminated samples after keeping the reaction vesicles in dark for 24 h did not

indicate bacterial growth. The synthesized composite powder causes irreversible damage of the bacterial cells not only in the presence, but in the absence of UV light. These experiments are visually illustrated in Figure 7. The picture shows the viable colonies on Mueller-Hinton agar (MHA) plates in undiluted, 10^{-1} and 10^{-2} diluted samples, respectively.

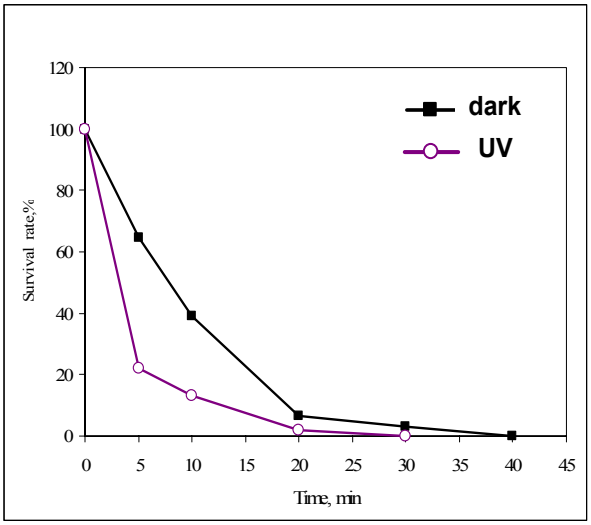

Fig. 6. Survival curves of Escherichia coli ATCC 25922 in presence of Ag/ZnO/$ZnTiO_3$ in dark and under UV radiation

It can be observed, that the number of colonies of *E. coli* progressively decreases from 10^5 CFU/ml at 5 min to 10^3 CFU/ml at 20 min and completely disappears at 40 min. According to our previous studies for antibacterial activities of nanosized $ZnTiO_3$ obtained by aqueous (aq) and nonaqueous (n-aq) sol-gel method, both illuminated samples destroyed about 99% of *E. coli* cells within 60 min [81, 82]. The as prepared more complex composite exhibited better properties compared to pure $ZnTiO_3$ powders. These results are compatible with those published in the literature. For comparison, Pant et al. [75] found that the Ag/TiO_2/ZnO powders killed the gram-negative *E. coli* bacteria under mild UV irradiation in 80 minutes. On the other hand, Nikam et al. [77] testing the antimicrobial activity against gram positive microorganism *Bacillus subtilis* and established that the Ag@Zn_2TiO_4 sample possesses higher antimicrobial activity compared to the undoped Zn_2TiO_4 sample.

On the basis of the obtained results we suggested a simple scheme for synthesis of composites. The preparation route consists of three main stages: i) sol-gel synthesis; ii) calcinations (300-400^{0}C) and iii) solid state reaction at 500-600^{0}C.

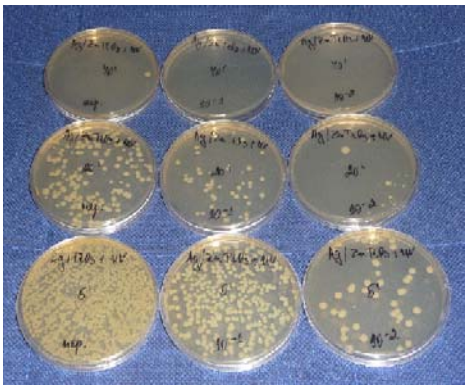

Fig. 7. Growth of Escherichia coli ATCC 25922 on Mueller-Hinton agar plates after treatment with illuminated Ag/ZnO/$ZnTiO_3$

4. Conclusions

A composite was obtained in the Ag/TiO_2/ZnO system by sol-gel method using titanium ethoxide, zinc acetate and citric acid as main precursors. It was established that at the lower temperature (300-400^{0}C) the obtained composite contains amorphous phase, elementary silver and ZnO. The heat treatment at 600^{0}C led to phase transformation of initial composition Ag/TiO_2/ZnO (atomic ratio 1:2:3) into a composite Ag/ZnO/$ZnTiO_3$, containing three active phases. This new composite material possesses good photocatalytic activity against Malachite green organic dye under UV irradiation. It showed strong antimicrobial activities toward high concentration of *E. coli* bacteria and completely killed them in 30 min in presence and absence of UV irradiation. The obtained material could be potentially applied in the disinfection practice.

Acknowledgements

The author Ahmed Shalaby thanks to the Erasmus Mundus MEDASTAR (Mediterranean Area for Science Technology and Research) Program. Authors are also grateful to the support of Medical University-Pleven, Contract No10/2013 for the performance of photocatalytic and antibacterial properties.

References

[1] O. Carp, C. Z. Huisman, A. Reller, Progress in solid state chemistry, **32**, 33 (2004).
[2] A. L. Linsbigler, G.Q. Lu, J. T. Yates, Chem. Rev., **95,** 735 (1995).
[3] K. Tanaka, M. Capule, T. Hisanaga, Chem. Phys. Lett., **187**, 73 (1991).

[4] S. Sakka, Processing, characterization and applications, vol. I, ed. H. Kozuka, Kluwer Acad. Publishers, 2005, Boston-Dordrecht-London.
[5] A. Fujishima, T. Rao, D. Tryk, J. Photochem. Photobiol. C: Photochem. Rev., 1, 1 (2000).
[6] M. Chong, B. Jin, C. Chow, C. Saint, Water Res. **44** (2010) 2997-3027.
[7] H. Markos, U. Ozgur, Zink oxide, Fundamentals, Materials and device Technology, Wiley-VCH, Verlag Gmbh & Co. KgaA. 2009.
[8] J. A. Rodriguez, M. Garcia, Synthesis Properties and Applications of oxide nanomaterials, chap. 17, Nanostructured oxides in photo catalysis, John Wiley & Sons Inc. 2007
[9] C. Hariharan, Applied Catalysis. A: General **304**, 55 (2006).
[10] D. Li, H. Haneda, N. Ohashi, S. Hishite, Catal. Today, **93-95,** 895 (2004).
[11] Y. Jang, C. Simer, T. Ohm, Mater. Res. Bull., **41**, 67 (2006).
[12] R. Comparelli, E. Fanizza, M. L. Curri, P. D. Cozzoli, G. Mascolo, A. Agostiano, Appl. Catalysis B: Environmental, **55**(2), 81 (2005).
[13] C. Marci, V. Augugliaro, M. Z. Lopez-Munoz, C. Martin, L. Palmisano, V. Rives, M. Schiavello, R. J. D. Tilley, A. M. Venezia, J. Phys. Chem. B, **105,** 1033 (2001).
[14] F. H. Dulin, D. E. Rase, J. Amer. Ceram. Soc., **43**, 125 (1960).
[15] O. Yamaguchi, M. Morimi, H. Kawabata, K. Shimizu, J. Amer. Ceram. Soc., **70**, c97 (1987).
[16] Y. S. Chang, Y. H. Chang, I. G. Chen, G. J. Chen, Y. L. Chai, T. H. Fang, S. Wu, Ceram. Intern., **30,** 2183 (2004).
[17] V. Parvanova, I. Illiev, L. Ilkov, J. Chem. Technol. Metall., **11**, 461 (2006).
[18] N. Obradovic, N. Mitrovic, V. Pavlovic, Ceram. Intern., **85,** 35 (2009).
[19] M. R. Mohammadi, D. Fray, J. Europ. Cer. Soc., **30**, 947 (2010).
[20] I. Bobowska, A. Opasinska, A. Wypych, P. Wojciechowski, Mater. Chem. Phys., **134,** 87 (2012).
[21] H. T. Kim, S. Nahm, J. D. Bynn, J. Amer. Cer. Soc., **82**, 3476 (1999).
[22] G. Liu, G. Li, X. Qui, et al., J. Alloys Compds, **481,** 492 (2009).
[23] Ji Kong, A. Li, H. Zhai, et al., J. Hazard. Mater., **171**, 918 (2009).
[24] N. Pal, M. Paul, A. Bhaumik, Appl. Cat. A: General, **383**, 153 (2011).
[25] B. C. Yadav, A. Yadav, S. Singh, K. Singh, Sensors and Actuators B: Chemical, **177**, 605 (2013).
[26] Y. S. Chang, Y. H., Chang, L. G. Chen, G. J. Chen, Y. I. Chai, J. Cryst. Growth, **243**, 319 (2002).
[27] L. L. Zhao, F. Q. Ziu, X. W. Wang, Z. Y. Zhang, L. F. Yan, J. Sol-Gel Sci. Technol., **33**, 103 (2005).
[28] N. Nolan, M. Seery, S. Pillai, Chem. Mater. **23**, 1496 (2011).
[29] Y. W. Wang, P. H. Yuan, C. M. Fan, Y. Wang, G. Y. Ding, Y. F. Wang, Ceram. Inter. **38,** 4173 (2012).
[30] Y. H. Yu, M. Xia, Mater. Lett., **77**, 10 (2012).
[31] A. Chaouchi, M. Saidai, S. d'Astorg, S. Marinel, Proccessing and Application of Ceramics **6**, 83 (2012).
[32] A. Bojinova, Tz. Dushkin, Bulg. J. Chem., **1**(2), 95 (2012) (in Bulgarian).
[33] F. Han, V. Kambala, M. Srinivasan, D. Rajarathnam, R. Naidu, Appl. Cat. A: General **359,** 25 (2009).
[34] H. Chao, Y. Yun, H. Xingfang, A. Larbot, J. Europ. Cer. Soc., **23,** 1457 (2003).
[35] H. Sung-Suh, J. Choi, H. Hah, S. Koo, Y. Bae, J. Photochem. Photobiol. A: Chem, **163**, 37 (2004).
[36] X. Qi, Z. Wang, Y. Zhuang, Y. Yu, J. L. Li, J. Hazard. Mater., **118**, 219 (2005).
[37] M. Seery, R. George, P. Floris & S. Pillai, J. Photochem. Photobiol. A: Chem., **189**, 258 (2007).
[38] Sh. Ansari Amin, M. Pazouki and A. Hosseinnia, Powder Technol., **196**, 241 (2009).
[39] Z. Wen, L. Tian-Mo, L. De-Jun, Phys. B, **405,** 4235 (2010).
[40] H. Li, G. Zhao, Z. Chen, B. Song, G. Han, J. Am. Ceram. Soc., **93**(2), 445 (2010).
[41] P. Wu, R. Xie, K. Imlay, J. K. Shang, Environm. Sci. Technol., **44,** 6992 (2010).
[42] P. Peerakiatkhajohn, W. Onreabroy, C. Chawengkijwanich, S. Chiarakorn, J. Sustainable Energy & Environ., **2**, 121 (2011) -125.
[43] K. Gupta, R. Singh, A. Pandey, A. Pandey, Beilstein J. Nanotechnol., **4,** 345 (2013).
[44] M. Viana, N. Mohallem, D. Miquita, K. Balzuweit, E. Silva-Pinto, Appl. Surf. Sci., **265,** 130 (2013).
[45] F. Petronella, S. Diomede, E. Fanizza, G. Mascolo, T. Sibillano, A. Agostiano, M. L. Curri, R. Comparelli, Chemosphere, **91**, 941 (2013).
[46] J. W. Yoon, T. Sasaki, N. Koshizaki, E. Traversa, Scripta Mater, **44**, 1865 (2001).
[47] M. Sökmen, D. W. Allen, F. Akkaş, N. Kartal, F. Acar, Water, Air and Soil Pollution, **132**, 153 (2001).
[48] M. Behnajady, N. Modirshahla, M. Shokri, B. Rad, Global Nest Journal, **10**, 1 (2008).
[49] B. Tryba, M. Piszcz, A. Morawski, The Open Mater. Sci. J., **4**, 58 (2010).
[50] C. Yu, L. Wei, X. Li, J. Chen, Q. Fan, J. Yu, Mater. Sci. Engineer. B: Adv. Funct. Solid State Mater., **178**, 344 (2013).
[51] S. F. Chen, J. P. Li, K. Qian, W. P. Xu, Y. Lu, W. X. Huang, S. H. Yu, Nano Research, **3**, 244 (2010).
[52] M. Behpour, S. Ghoreishi, F. Razavi, Digest J. Nanomater. Biostruct., **5**, 467 (2010).
[53] K. Kaneko, Won-Jin Moon, K. Inoke, Z. Horita, S. Ohara, T. Adschiri, H. Abe, M. Naito, Mater. Sci. Engineer., A, **403**, 32 (2005).
[54] P. Zhang, C. Shao, X. Li, M. Zhang, X. Zhang, Y. Sun, Y. Liu, J. Hazard. Mater., **237-238,** 331 (2012).

[55] B. Aysin, J. Park, A. Ozturk, Production of silver loaded photocatalytic TiO_2 powders by ball milling, in Nanocon 2011, Slezska: Tanger Ltd, (2011) p. 521-527.
[56] M. Andersson, H. Birkedal, N. Franklin, T. Ostomel, S. Boettcher, A. Palmqvist, G. Stucky, Chem. Mater., **17**, 1409 (2005).
[57] C. Srinivasan & N. Somasundaram, Curr. Sci., **85**, 1431 (2003).
[58] J. H. Hsieh, R. B. Yu, Y. K. Chang, C. Li, Structural analysis of TiO_2 and TiO_2-Ag thin films and their antibacterial behaviors, In 4th International Symposium on Functional Materials. Bristol: Iop Publishing Ltd; 2012
[59] V. V. Shvalagin, A. L. Stroyuk, S. Ya. Kuchmii, Journal of Nanoparticle Research, **9**, 427 (2007).
[60] J.Yan, X. Sun, Y. Zhu, Y Zhao, Proc. of SPIE, **6624**, 662413 (2008).
[61] X. Y. Ye, Y. M. Zhou, Y. Q. Sun, J. Chen, Z. Q. Wang, J. Nanopart. Res., **11**, 1159 (2009).
[62] P. Bazant, I. Kuritka, M. Machovsky, T. Sedlacek, M. Pastorek, Microwave assisted synthesis of Ag-ZnO particles and their antibacterial properties. Mathematical Methods and Techniques in Engineering and Environmental Science, Catania, Italy, 3rd-5th September, 2011, ISBN: 978-1-61804-046-6, p. 341-346.
[63] C. Karunakaran, V. Rajeswari, P. Gomathisankar, J. Alloys Compds., **508**, 587 (2010).
[64] Ch. Ren, B. Yang, M. Wu, J. Xu, Zh. Fu, Y. Lv, T. Guo, Y. Zhao, C. Zhu, J. Hazard. Mater. **182**, 123 (2010).
[65] M. Machovsky, P. Bazant, Z. Kozakova, M. Pastorek, P. Žlebek, I. Kuritka, Nanocon, 2011, 21. – 23. 9. 2011, Brno, Czech Republic.
[66] A. Akbar Ashkarran, Appl. Phys. A, **107**, 401 (2012).
[67] G. Singh, E. M. Joyce, J. Beddow and T. J. Mason, J. Microbiol., Biotechnol. Food Sci. **2**(1), 106 (2012).
[68] K. Thongsuriwong, P. Amornpitoksuk, S. Suwanboon, J. Sol-Gel Sci. Technol. **62**, 304 (2012).
[69] A. H. Shah, E. Manikandan, M. Basheer Ahmed, V. Ganesan, J. Nanomed. Nanotechol., **4**(3), 1000168 (2013).
[70] T. Welderfael, O. P. Yadav, A. M. Taddesse, J. Kaushal, , Bull. Chem. Soc. Ethiop. **27**(2) 221 (2013).
[71] S. Azizi, M. B. Ahmad, M. Z. Hussein, N. A. Ibrahim, Molecules, **18**, 6269 (2013).
[72] S. Reddy, V. Reddy, K. N. Reddy, P. J. Kumari, Res. J. Mater. Sci., **1**(1), 11 (2013).
[73] S. Ansari, M. Khan, J. Lee, M. Cho, J. Industr. Engineer. Chem., (2013) in press.
[74] L. Collado, P. Jana, B. Sierra, J. M. Coronado, P. Pizarro, D. P. Serrano, V.A. de la Peña O'Shea, Chem. Engineer. J., **224**, 127 (2013).
[75] H. R. Pant, B. Pant, R. K. Sharma, A. Amarjargal, H. J. Kim, C. H. Park, L. D. Tijing, C. S. Kim, Ceram. Intern., **39** 1503 (2013).
[76] Y.-W. Chen, D.-S. Lee, H.-J. Chen, Intern. J. Hydrogen Energy, **37**, 15140 (2012).
[77] L. Nikam, R. Patil, R. Panmand, S. Kadam, K. Sivanandan, B. Kale, Adv. Sci. Engineer. Medicine, **5**(7), 688 (2013).
[78] B. Ohtani, J. Photochem. Photobiol. C: Photochem. Reviews, **11**, 157 (2010).
[79] Y. Dimitriev, Y. Ivanova, A. Staneva, L. Alexandrov, M. Mancheva, R. Yordanova, C. Dushkin, N. Kaneva, C. Iliev, J. Univ. Chem. Technol. Metall., **44**(3), 235 (2009).
[80] A. Shalaby, Y. Dimitriev, R. Iordanova, A. Bachvarova-Nedelcheva, Tz. Iliev, J. Univ. Chem. Technol. Metall., **46** (2), 137 (2011).
[81] A. Stoyanova, Y. Dimitriev, A. Shalaby, A. Bachvarova-Nedelcheva, R. Iordanova, M. Sredkova, J. Optoel. Biomed. Mater. **3**(1), 24 (2011).
[82] A. Stoyanova, A. Bachvarova-Nedelcheva, R. Iordanova, N. Ivanova, H. Hitkova, M. Sredkova, Digest J. Nanomater. Biostr., **7**(2), 777 (2012).
[83] A. Shalaby, A. Bachvarova-Nedelcheva, R. Iordanova, Y. Dimitriev, J. Chem. Techn. Metall., **48**(6), 585 (2013).
[84] A. Stoyanova, H. Hitkova, A. Bachvarova-Nedelcheva, R. Iordanova, N. Ivanova, M. Sredkova, J. Chem. Techn. Metall., **48**(2), 154 (2013).
[85] A. Bachvarova-Nedelcheva, R. Iordanova, A. Stoyanova, R. Gegova, Y. Dimitriev, A. Loukanov, Centr. Eur. J. Chem., **11**(3), 364 (2013).
[86] R. Gegova, Y. Dimitriev, A. Bachvarova-Nedelcheva, R. Iordanova, A. Loukanov, Tz. Iliev, J. Chem. Techn. Metall., 48(2), 147 (2013).
[87] R. Iordanova, A. Bachvarova-Nedelcheva, Y. Dimitriev, Tz. Iliev, Bulg. Chem. Commun., **43**(3), 378 (2011).
[88] N. Kaneva, G. Yordanov, C. Dushkin, Bull. Mater. Sci., **33**(2), 111 (2010).
[89] N. Kaneva, I. Stambolova, V. Blaskov, Y. Dimitriev, A. Bojinova, C. Dushkin, Surf. Coat. Techn., **207**, 5 (2012).
[90] A. Bojinova, R. Kralchevska, I. Poulios, C. Dushkin, Mater. Chem. Phys., **106**, 187 (2007).
[91] S. Siuleiman, N. Kaneva, A. Bojinova, K. Papazova, A. Apostolov, D. Dimitrov, Colloids Surf. A: Physicochem. Eng. Aspects (2014), http://dx.doi.org/10.1016/j.colsurfa.2014.01.010 (in press).
[92] W. Weng, G. Han, P. Du, G. Shen, Mater. Chem. Phys., **74**, 92 (2002).
[93] J. Dharma, A. Pisal, Perkin Elmer, Inc, Application note.
[94] M. Kanna, S. Wongnawa, Mater. Chem. Phys., **110**, 166 (2008).
[95] S. Buddee, S. Wongnawa, U. Sirimahachai, W. Puetpailbool, Mater. Chem. Phys., **126**, 167 (2011).

[96] A. Bojinova, C. Dushkin, Reac. Kinet. Mech. Catal., **103**, 239 (2011).
[97] Z. Zhang, P. Maggard, J. Photochem. Photobiol. A: Chem., **186**, 8 (2007).
[98] S. Tan, B. Chen, X. Sun, W. Fan, H. Kwok, X. Zhang, S. Chua, J. Appl. Phys., **98**, 013505-5 (2005).
[99] E. A. Meulenkamp, J. Phys. Chem. B, **102**, 5566 (1998).
[100] K. Naoi, Y. Ohko, T. Tatsuma, J. Am. Chem. Soc., **126**(11), 3664 (2004).
[101] K. Nagaveni, M. S. Hegde, N. Ravishankar, G. N. Subanna, G. Madras, Langmuir, **20**, 2900 (2004).
[102] S. Valencia, J. M. Marin, G. Restrepo, The Open Mater. Sci. J., **4**, 9 (2010).
[103] P. Khain, D. Kumar, A. Kumar, D. Kaur, Optoelectron. Adv. Mater. - Rapid Commun **4**(3), 299 (2010).
[104] C. Ye, Y. Wang, Y. Yo, J. Zhang, G. H. Li, J. Appl. Phys., **106**, 033520-4 (2009).
[105] K. Kaur, Ch. Singh, Energy Procedia, **29**, 291 (2012).

*Corresponding author: ashalaby@outlook.com; albenadb@svr.igic.bas.bg